Fast Frequency Response Calculations of Cavity-Backed Aperture Antennas Using Hybrid FEM/MoM Technique in Conjunction with Model Based Parameter Estimation

C. J. Reddy, *Hampton University*
M. D. Deshpande, *ViGYAN Inc.*
C. R. Cockrell and F. B. Beck, *NASA Langley Research Center*
Hampton VA 23681

ABSTRACT

Model Based Parameter Estimation (MBPE) is presented in conjunction with the hybrid Finite Element Method (FEM)/Method of Moments (MoM) technique for fast computation of the input characteristics of cavity-backed aperture antennas over a frequency range. The hybrid FEM/MoM technique is used to form an integro-partial-differential equation to compute the electric field distribution of a cavity-backed aperture antenna. In MBPE, the electric field is expanded as a rational function of two polynomials. The coefficients of the rational function are obtained using the frequency derivatives of the integro-partial-differential equation formed by the hybrid FEM/MoM technique. Using the rational function approximation, the electric field is calculated and the input characteristics of the antenna are obtained over the frequency range. Numerical results for an open coaxial line and a cavity-backed microstrip patch antenna are presented. Good agreement between MBPE and the solutions over individual frequencies is observed. CPU timings for all numerical calculations are presented.

1 INTRODUCTION

Cavity-backed aperture antennas are very popular in aerospace applications due to their conformal nature. Hybrid techniques have become attractive for numerical analysis of these type of problems due to their ability to handle arbitrary shape of the cavity and complex materials that may be required for the antenna design. The combined Finite Element Method (FEM) and Method of Moments (MoM) technique in particular has been used to analyze various cavity-backed aperture antennas [1,2]. In the combined FEM/MoM technique, FEM is used in the cavity volume to compute the electric field, whereas MoM is used to compute the magnetic current at the aperture. Using Galerkin's technique, an integro-partial-differential equation is formed. The cavity is divided into tetrahedral elements and the aperture is discretized by triangles. Simultaneous equations are generated over the subdomains and are added to form a global matrix equation. This results in a partly sparse and partly dense symmetric complex matrix, which can be solved either by a direct solver or by an iterative solver. The electric field hence obtained is used to compute the radiation characteristics and input characteristics of the antenna.

In most practical applications, input characteristics such as input impedance or input admittance are of interest over a frequency range. To obtain the frequency response of the antenna, one has to repeat the above calculations at every incremental frequency over the frequency band of interest. If the antenna is highly frequency dependent, one needs to do the calculations at fine increments of frequency to get an accurate representation of the frequency response. For electrically large cavities with large apertures, this can be computationally intensive and in some cases computationally prohibitive. Model Based Parameter Estimation (MBPE) was proposed by Miller and Burke [3] to alleviate the above problems in frequency domain electromagnetics. In [3,4], the applicability of MBPE to computing frequency response for various electromagnetic problems and particularly to the NEC code [5] for efficient computation of input characteristics of wire antennas over a wide frequency range was demonstrated.

In this paper, MBPE is applied for predicting the input characteristics of cavity-backed aperture antennas over a frequency range using the combined FEM/MoM technique. In MBPE technique, the electric field is expanded as a rational function. The coefficients of the rational function are obtained using the frequency data and the frequency derivative data. Once the coefficients of the rational function are obtained the electric field in the cavity can be obtained at any frequency within the frequency range. Using the electric field, the input characteristics such as the input impedance or admittance can be calculated. If the frequency derivative information is known for more than one frequency, a rational function matching the frequency data and frequency derivative data at all frequencies, can be obtained resulting in a broad frequency response.

The rest of the paper is organized as follows. In section 2, MBPE implementation for the combined FEM/MoM technique is described. Numerical results for an open coaxial line and a cavity-backed microstrip patch antenna are presented in section 3. The numerical data are compared with the exact solution over the frequency range. CPU

Manuscript Received 20th February 1998.
C. J. Reddy, email: *c.j.reddy@larc.nasa.gov*

timings are given for each example. Concluding remarks on the advantages and disadvantages of MBPE are given in section 4.

2 MBPE IMPLEMENTATION FOR THE COMBINED FEM/MoM TECHNIQUE

The geometry of the problem to be analyzed is shown in figure 1. For linear, isotropic, and source free region, the electric field satisfies the vector wave equation:

$$\nabla\times\left(\frac{1}{\mu_r}\nabla\times\mathbf{E}\right)-k^2\varepsilon_r\mathbf{E}=0 \tag{1}$$

where μ_r, ε_r are the relative permeability and relative permittivity of the medium in the cavity and k is the free space wavenumber at any frequency f. The time variation $\exp(j\omega t)$ is assumed and suppressed throughout this report. Applying the Galerkin's technique, equation (1) can be written in "weak form" as [1]

$$\iiint_V\left[(\nabla\times\mathbf{T})\bullet\left(\frac{1}{\mu_r}\nabla\times\mathbf{E}\right)-k^2\varepsilon_r\mathbf{T}\bullet\mathbf{E}\right]dv - j\omega\mu_o\int\int_{S_{ap}}(\mathbf{T}\times\hat{\mathbf{n}}_a)\bullet\mathbf{H}_{ap}ds = j\omega\mu_o\int\int_{S_{inp}}\mathbf{T}\bullet(\hat{\mathbf{n}}_i\times\mathbf{H}_{inp})ds \tag{2}$$

where $\mathbf{T}$ is the vector testing function, S_{ap} is the aperture surface, and S_{inp} is the input surface (see figure 1). $\mathbf{H}_{ap}$ is the magnetic field at the aperture and $\mathbf{H}_{inp}$ is the magnetic field at the input surface. $\hat{\mathbf{n}}_a$ and $\hat{\mathbf{n}}_i$ are the unit normals to the surfaces S_{ap} and S_{inp}, respectively.

In accordance with the equivalence principle [9], the fields inside the cavity can be decoupled to the fields outside the cavity by closing the aperture with a Perfect Electric Conductor (PEC) and introducing the equivalent magnetic current.

$$\mathbf{M}=\mathbf{E}\times\hat{\mathbf{n}}_a \tag{3}$$

over the extent of the aperture. Making use of the image theory, the integrals over S_{ap} in equation (2) can be written as

$$j\omega\mu_o\int\int_{S_{ap}}(\mathbf{T}\times\hat{\mathbf{n}}_a)\bullet\mathbf{H}_{ap}ds = \frac{k^2}{2\pi}\int\int_{S_{ap}}\mathbf{T}_s\bullet\left(\int\int_{S_{ap}}\mathbf{M}\frac{\exp(-jkR)}{R}ds'\right)ds - \frac{1}{2\pi}\int\int_{S_{ap}}(\nabla\bullet\mathbf{T}_s)\left\{\int\int_{S_{ap}}(\nabla'\bullet\mathbf{M})\frac{\exp(-jkR)}{R}ds'\right\}ds \tag{4}$$

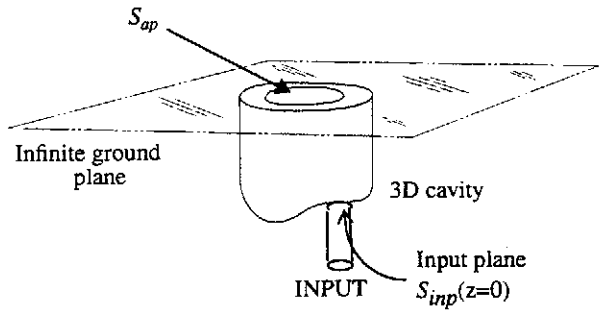

Figure 1 Geometry of cavity-backed aperture in an infinte ground plane.

where $\mathbf{T}_s=\mathbf{T}\times\hat{\mathbf{n}}_a$ and R is the distance between source point and the observation point. ∇' indicates del operation over the source coordinates and ds' indicates the surface integration over the source region.

Though the analysis presented in this report is not limited to any specific input feed structure, we restrict the presentation of the formulation to the coaxial line as the input feed structure. The cross section of the coaxial line is shown in figure 2. Assuming that the incident electric field is the transverse electromagnetic (TEM) mode and the reflected field also consists of TEM mode only, the electric field at the input plane S_{inp} is given by

$$\mathbf{E}_{inp}=\mathbf{e}_{inc}\exp(-jk\sqrt{\varepsilon_{rc}}z)+\mathbf{e}_{ref}\exp(jk\sqrt{\varepsilon_{rc}}z) \tag{5}$$

where

$$\mathbf{e}_{inc}=\hat{\rho}\frac{1}{\sqrt{2\pi\ln\left(\frac{r_2}{r_1}\right)}}\frac{1}{\rho} \tag{6}$$

and

$$\mathbf{e}_{ref}=R_o\mathbf{e}_{inc} \tag{7}$$

R_o is the reflection coefficient at $z=z_1$ and is given by

$$R_o=\frac{\exp(-jk\sqrt{\varepsilon_{rc}}z_1)}{\sqrt{2\pi\ln\left(\frac{r_2}{r_1}\right)}}\int\int_{S_{inp}}\mathbf{E}\bullet\left(\frac{\hat{\rho}}{\rho}\right)ds-\exp(-2jk\sqrt{\varepsilon_{rc}}z_1) \tag{8}$$

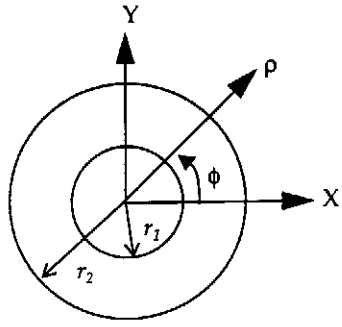

Figure 2 Cross section of the coaxial line.

r_2 is the outer radius and r_1 is the inner radius of the coaxial line. ε_{rc} is the relative permittivity of the coaxial line.

Using equation (5) to calculate $\mathbf{H}_{inp}$, the surface integral over S_{inp} in equation (2) can be written as

$$j\omega\mu_o\int\int_{S_{inp}} \mathbf{T}\bullet(\hat{\mathbf{n}}_i\times\mathbf{H}_{inp})ds = \frac{-jk\sqrt{\varepsilon_{rc}}}{2\pi\ln\left(\frac{r_2}{r_1}\right)\mu_{rc}}\left\{\int\int_{S_{inp}}\mathbf{T}\bullet\left(\frac{\hat{\rho}}{\rho}\right)ds\right\}\left\{\int\int_{S_{inp}}\mathbf{E}\bullet\left(\frac{\hat{\rho}}{\rho}\right)ds\right\} + \frac{2jk\sqrt{\varepsilon_{rc}}\exp(-jk\sqrt{\varepsilon_{rc}}z_1)}{\mu_{rc}\sqrt{2\pi\ln\left(\frac{r_2}{r_1}\right)}}\int\int_{S_{inp}}\mathbf{T}\bullet\left(\frac{\hat{\rho}}{\rho}\right)ds \quad (9)$$

μ_{rc} is the relative permeability of the coaxial line. Substituting equation (4) and (9) in equation (2), the system equation for the combined FEM/MoM technique can be written as

$$\begin{aligned}&\iiint_V\left[(\nabla\times\mathbf{T})\bullet\left(\frac{1}{\mu_r}\nabla\times\mathbf{E}\right)-k^2\varepsilon_r\mathbf{T}\bullet\mathbf{E}\right]dv\\ &-\frac{k^2}{2\pi}\int\int_{S_{ap}}\mathbf{T}_s\bullet\left(\int\int_{S_{ap}}\mathbf{M}\frac{\exp(-jkR)}{R}ds'\right)ds\\ &+\frac{1}{2\pi}\int\int_{S_{ap}}(\nabla\bullet\mathbf{T}_s)\left\{\int\int_{S_{ap}}(\nabla'\bullet\mathbf{M})\frac{\exp(-jkR)}{R}ds'\right\}ds\\ &+\frac{jk\sqrt{\varepsilon_{rc}}}{2\pi\ln\left(\frac{r_2}{r_1}\right)\mu_{rc}}\left\{\int\int_{S_{inp}}\mathbf{T}\bullet\left(\frac{\hat{\rho}}{\rho}\right)ds\right\}\left\{\int\int_{S_{inp}}\mathbf{E}\bullet\left(\frac{\hat{\rho}}{\rho}\right)ds'\right\}\\ &=\frac{2jk\sqrt{\varepsilon_{rc}}\exp(-jk\sqrt{\varepsilon_{rc}}z_1)}{\mu_{rc}\sqrt{2\pi\ln\left(\frac{r_2}{r_1}\right)}}\int\int_{S_{inp}}\mathbf{T}\bullet\left(\frac{\hat{\rho}}{\rho}\right)ds\end{aligned} \quad (10)$$

The volume of the cavity is subdivided into small volume tetrahedral elements. The electric field is expressed in terms of the edge vector basis functions [7], which enforce the divergenceless condition of the electric field as

$$\mathbf{E}=\sum_{i=1}^{6}e_i\mathbf{W}_i \quad (11)$$

The vector testing function is also expressed in terms of the edge vector basis functions following the Galerkin's method. The discretization of the cavity volume into tetrahedral elements automatically results in discretization of the surfaces S_{ap} and S_{inp} into triangular elements. The magnetic current at the radiating aperture S_{ap} can be expressed in terms of unknown coefficients associated with the tetrahedral elements as

$$\mathbf{M}=\sum_{i=1}^{3}e_i\mathbf{W}_{si} \quad (12)$$

where $\mathbf{W}_{si}=\mathbf{W}_i\times\hat{\mathbf{n}}_a$. The volume and surface integrals in equation (10) are carried out over each element to form element matrices and the element matrices are assembled to form global matrices. Equation (10) can be written in matrix form as

$$A(k)e(k)=B(k) \quad (13)$$

$A(k)$ is a partly sparse, partly dense complex symmetric matrix, $B(k)$ is the excitation vector, and $e(k)$ is the unknown electric field coefficient vector. $A(k)$ can be written as a sum of four matrices

$$A(k)=A_1(k)+A_2(k)+A_3(k)+A_4(k) \quad (14)$$

where

$$A_1(k)=\sum_{jt=1}^{6}\iiint_{mt}\left[(\nabla\times\mathbf{W}_{it}^{(mt)})\bullet\left(\frac{1}{\mu_r}\nabla\times\mathbf{W}_{jt}^{(mt)}\right)-k^2\varepsilon_r\mathbf{W}_{it}^{(mt)}\bullet\mathbf{W}_{jt}^{(mt)}\right]dv$$

$$mt=1,2,3,....N_v;\ \ it=1,2,3,4,5,6 \quad (15)$$

$$A_2(k)=\sum_{pt=1}^{N_a}\left[\sum_{lt=1}^{3}\left\{-\frac{k^2}{2\pi}\int\int_{nt}\mathbf{W}_{s(kt)}^{(nt)}\bullet\left(\int\int_{pt}\mathbf{W}_{s(lt)}^{(pt)}\frac{\exp(-jkR)}{R}ds'\right)ds\right\}\right]$$

$$nt=1,2,3,....N_a;\ \ kt=1,2,3 \quad (16)$$

$$A_3(k)=\sum_{pt=1}^{N_a}\left[\sum_{lt=1}^{3}\left\{\frac{1}{2\pi}\int\int_{nt}(\nabla\bullet\mathbf{W}_{s(kt)}^{(nt)})\int\int_{pt}(\nabla'\bullet\mathbf{W}_{s(lt)}^{(pt)})\frac{\exp(-jkR)}{R}ds'ds\right\}\right]$$

$$nt=1,2,3,....N_a;\ \ kt=1,2,3 \quad (17)$$

$$A_4(k)=\frac{jk\sqrt{\varepsilon_{rc}}}{2\pi\ln\left(\frac{r_2}{r_1}\right)\mu_{rc}}\left[\sum_{rt=1}^{N_i}\left\{\sum_{yt=1}^{3}\left(\int\int_{qt}\mathbf{W}_{xt}^{(qt)}\bullet\left(\frac{\hat{\rho}}{\rho}\right)ds\right)\left(\int\int_{rt}\mathbf{W}_{yt}^{(rt)}\bullet\left(\frac{\hat{\rho}}{\rho}\right)ds'\right)\right\}\right]$$

$$qt=1,2,3,.....N_i;\ xt=1,2,3 \quad (18)$$

and

$$B(k)=\frac{2jk\sqrt{\varepsilon_{rc}}\exp(-jk\sqrt{\varepsilon_{rc}}z_1)}{\mu_{rc}\sqrt{2\pi\ln\left(\frac{r_2}{r_1}\right)}}\int\int_{qt}\mathbf{W}_{xt}^{(qt)}\bullet\left(\frac{\hat{\rho}}{\rho}\right)ds$$

$$qt=1,2,3,.....N_i;\ xt=1,2,3 \quad (19)$$

N_v is the total number of tetrahedral elements in the volume of the cavity, N_a is the total number of triangles in the radiating aperture surface and N_i is the total number of triangles in the input surface.

The matrix equation (13) is solved at any specific frequency, f_o (with free space wavenumber $k_o = 2\pi f_o$) for the unknown electric field coefficients, which are used to obtain the electric field distribution. Once the electric field distribution is known, the input reflection coefficient can be calculated using equation (8) at the input plane S_{inp} with $z_1 = 0$ as

$$\Gamma = \frac{1}{\sqrt{2\pi \ln\left(\frac{r_2}{r_1}\right)}} \int\int_{S_{inp}} \mathbf{E} \bullet \left(\frac{\hat{\rho}}{\rho}\right) ds - 1 \tag{20}$$

The normalized input admittance at S_{inp} is given by

$$Y_{in} = \frac{1-\Gamma}{1+\Gamma} \tag{21}$$

The input admittance given in equation (21) is calculated at one frequency. If one needs the input admittance over a frequency range, this calculation is to be repeated at different frequency values. Instead MBPE [3,4] can be applied for rapid calculation of input admittance/ impedance over a frequency range. MBPE technique involves expanding the unknown coefficient vector as a rational function. The coefficients of the rational function are obtained by matching the function and its frequency derivatives of the function at one or more frequency points.

The solution of equation (13) at any frequency f_o gives the unknown electric field coefficient column vector $e(k_o)$. Instead $e(k)$ can be written as a rational function,

$$e(k) = \frac{P_L(k)}{Q_M(k)} \tag{22}$$

where

$$P_L(k) = a_o + a_1 k + a_2 k^2 + a_3 k^3 + \ldots\ldots\ldots\ldots + a_L k^L$$

$$Q_M(k) = b_o + b_1 k + b_2 k^2 + b_3 k^3 + \ldots\ldots\ldots\ldots + b_M k^M$$

b_o is set to 1 as the rational function can be divided by an arbitrary constant. The coefficients of the rational function are obtained by matching the frequency derivatives of $e(k)$. If equation (22) is differentiated t times with respect to k, the system of $(t+1)$ equations provides the information from which the rational function coefficients can be found if $t \geq L + M$. If the frequency derivatives are available at only one frequency f_o, the variable in the rational function can be replaced with $(k - k_o)$ *i.e.*,

$$e(k) = \frac{P_L(k-k_o)}{Q_M(k-k_o)} \tag{23}$$

and the derivatives can be evaluated at $k = k_o$. The coefficients of the rational function can be obtained from the following equations:

$$a_o = e(k_o) \tag{24}$$

$$\begin{bmatrix} 1 & 0 & 0 & \ldots & 0 & -e_o & 0 & \ldots & 0 \\ 0 & 1 & 0 & \ldots & 0 & -e_1 & -e_o & \ldots & 0 \\ 0 & 0 & 1 & \ldots & 0 & -e_2 & -e_1 & \ldots & 0 \\ \ldots & \ldots & \ldots & \ldots & \ldots & \ldots & \ldots & \ldots & \ldots \\ 0 & 0 & 0 & \ldots & 1 & -e_{L-1} & -e_{L-2} & \cdots & -e_{L-i} \\ 0 & 0 & 0 & 0 & 0 & -e_L & -e_{L-1} & \cdots & -e_{L-i+1} \\ 0 & 0 & 0 & 0 & 0 & -e_{L+1} & -e_L & \ldots & -e_{L-i+2} \\ \ldots & \ldots & \ldots & \ldots & \ldots & \ldots & \ldots & \ldots & \ldots \\ 0 & 0 & 0 & 0 & 0 & -e_{L+M-1} & -e_{L+M-2} & \cdots & -e_L \end{bmatrix} \begin{bmatrix} a_1 \\ a_2 \\ a_3 \\ \ldots \\ a_L \\ b_1 \\ b_2 \\ \ldots \\ b_M \end{bmatrix} = \begin{bmatrix} e_1 \\ e_2 \\ e_3 \\ \ldots \\ e_L \\ e_{L+1} \\ e_{L+2} \\ \ldots \\ e_{L+M} \end{bmatrix} \tag{25}$$

where $e_m = \frac{e^{(m)}}{m!}$ and $i=min(L,M)$.

This approach is same as the Padé approximation given in [8]. This method has been successfully applied to electromagnetic scattering from cavity-backed apertures using a hybrid FEM/MoM technique [9].

If the frequency derivatives are known at more than one frequency, then the expansion about $k=k_o$ should not be used and the system matrix to solve the rational function coefficients takes a general form [3]. For the sake of simplicity, only a two frequency model is presented here. Assume that at two frequencies, f_1 (with free space wavenumber k_1) and f_2 (with free space wavenumber k_2), four derivatives are evaluated at each frequency. Hence ten samples of data are available (two frequency samples and a total of eight frequency derivative samples) to form a rational function with $L=5$ and $M=4$

$$e(k) = \frac{a_o + a_1 k + a_2 k^2 + a_3 k^3 + a_4 k^4 + a_5 k^5}{1 + b_1 k + b_2 k^2 + b_3 k^3 + b_4 k^4} \tag{26}$$

Equation (26) can be written as

$$(1 + b_1 k + b_2 k^2 + b_3 k^3 + b_4 k^4) e(k) = a_o + a_1 k + a_2 k^2 + a_3 k^3 + a_4 k^4 + a_5 k^5 \tag{27}$$

Differentiating equation (27) four times at each frequency and writing a matrix equation, the coefficients of the rational function in equation (26) are obtained. In this procedure, $e^{(t)}$, the t^{th} derivative is obtained by taking derivatives of equation (13), which results in a recursive relationship [6,10],

$$e^{(t)} = A^{-1}(k)\left[B^{(t)} - \sum_{q=0}^{t}(1-\delta_{qo})C_{t,q}A^{(q)}(k)e^{(t-q)}(k)\right] \quad (28)$$

$A^{(q)}(k)$ is the q^{th} derivative of $A(k)$ with respect to k and $B^{(t)}(k)$ is the t^{th} derivative of $B(k)$ with respect to k. $C_{t,q} = \frac{t!}{q!(t-q)!}$. The Kronecker delta δ_{qo} is defined as

$$\delta_{qo} = \begin{cases} 1 & q = 0 \\ 0 & q \neq 0 \end{cases} \quad (29)$$

The frequency derivatives of $A(k)$ and $B(k)$ are evaluated [11] and are given in the appendix.

The above procedure can be generalized for multiple frequencies with frequency derivatives evaluated at each frequency to increase the accuracy of the rational function. Alternatively, the two-frequency-four-derivative model can be used with multiple frequency windows. The complexity of the matrix equation to solve for multiple-frequency-multiple derivative model increase with the number of frequency points and the number of derivatives taken at each frequency. The two-frequency-four-derivative model is followed in this paper.

3 NUMERICAL RESULTS

To validate the analysis presented in the previous sections, calculation of input characteristics over a frequency range are done for an open coaxial line and a cavity-backed square microstrip patch antenna. The numerical data obtained using MBPE are compared with the results calculated at each frequency using the computer code CBS3DR [12], which implements the combined FEM/MoM technique [2]. We will refer to the latter method as "exact solution". A percentage error is calculated as compared to the exact solution as

$$\%\ \text{error} = \left\| \frac{(MBPE\ Value - Exact\ Value)}{Exact\ Value} \right\| \times 100 \quad (30)$$

Due to the hybrid FEM/MoM technique, matrix $A(k_o)$ is partly sparse and partly dense. The Complex Vector Sparse Solver (CVSS) [13] is used to LU factor the matrix $A(k_o)$ once and the moments are obtained by backsolving equation (28) with multiple right-hand sides. All the computations reported below are done on SGI *Indigo2* (with IP22 processor) computer.

(a) Open Coaxial line:

An open coaxial line radiating into an infinite ground plane (figure 3a) is considered. A finite length of the line is used for FEM discretization. The input plane S_{inp} is placed at $z = 0$ plane and the radiating aperture at $z = 1cm$. The discretization of the coaxial line resulted in 1119 total unknowns, and the order of the dense matrix due to MoM is

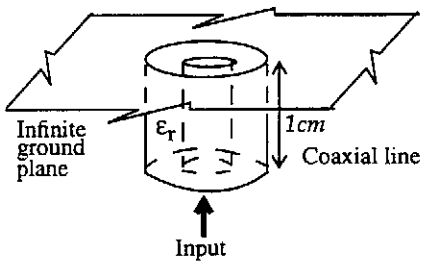

(a)

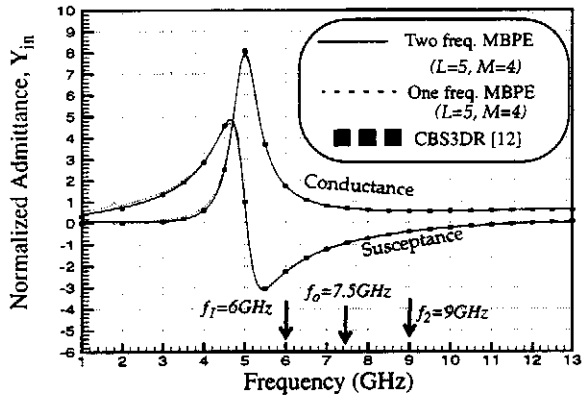

(b)

Figure 3 (a) Open coaxial line in an infinite ground plane. Inner radius r_1=1cm, Outer radius r_2=1.57cm and ε_{rc}=1.0
(b) Normalized input admittance as a function of frequency.

144. One-frequency MBPE with $L=5$ and $M=4$ at f_o=7.5GHz is used to calculate the frequency response of the input admittance. Two-frequency MBPE at f_1=6GHz and f_2=9GHz with $L=5$ and $M=4$ is also used to calculate the frequency response. The frequency response over the frequency range 1GHz-13GHz is plotted in figure 3(b) along with the exact solution calculated at 23 discrete frequency points over this frequency range. Both one-frequency and two-frequency MBPE frequency responses are calculated at 0.1GHz increments. The one-frequency MBPE resulted in an error of 0.037% for conductance and 0.45% for susceptance at 6GHz and at 9GHz, it resulted in an error of 0.08% for conductance and 0.027% for susceptance. The two-frequency MBPE resulted in an error of 0.5% for conductance and 0.2% for susceptance at 7.5GHz. The exact solution took 990 secs to calculate input admittance at 23 frequency values from 1GHz to 13GHz. It can be seen that one-frequency MBPE agrees well with the exact solution over the frequency range 4.5GHz to 13GHz, whereas two-frequency MBPE agrees well with the exact solution over the frequency range 1GHz to 13GHz. Both one-frequency MBPE and two-frequency are faster than the exact solution over the frequency range. Two-frequency MBPE has advantage over the one-frequency MBPE as it requires less computer memory[1].

1. Please see the comment on storage at the end of this section for detailed explanation.

(b) Cavity-Backed Square Microstrip Patch Antenna:

A cavity-backed square microstrip antenna radiating into an infinite ground plane (figure 4a) is considered. The input plane S_{inp} is placed at $z = 0$ plane and the radiating aperture at $z = 0.16cm$. The discretization of the cavity volume resulted in 2,160 total unknowns and the order of the dense matrix due to MoM is 544. The frequency response of the input impedance $(1/Y_{in})$ is calculated using one-frequency MBPE with L=5 and M=4 at f_0=4GHz and also using two-frequency MBPE with L=5 and M=4 at f_1=3GHz and f_2=5GHz. The numerical data is plotted in figure 4b along with the exact solution calculated at 23 frequency points over the frequency range 1GHz to 7GHz. The one-frequency MBPE calculations resulted in an error of 5.4% for resistance and 0.28% for reactance at 3GHz and an error of 1.79% for resistance and 0.93% for reactance at 5GHz.

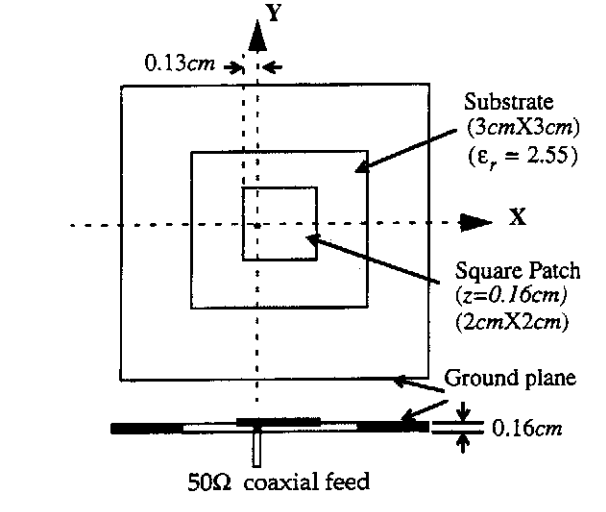

(a)

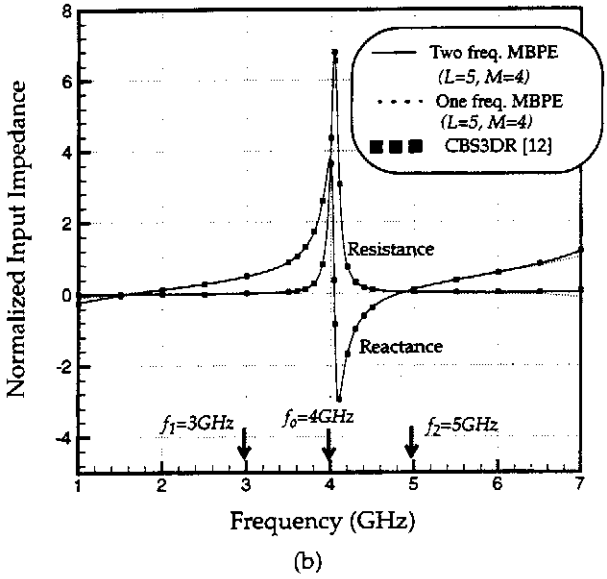

(b)

Figure 4 (a) Cavity-backed square microstrip patch antenna in an infinite ground plane fed by a 50Ω coaxial line.

(b) Normalized input impedance versus frequency

The two-frequency MBPE has an error of 0.3% for resistance and 0.36% for reactance at 4GHz. Both one-frequency and two-frequency MBPE frequency responses are calculated with 0.01GHz increments. One-frequency MBPE took 1107secs of CPU time to generate the moments, whereas the two-frequency MBPE took a total of 1120 secs of CPU time to generate moments at both frequencies. The exact solution took a total of 11,891 secs of CPU time for computations at 23 frequency points over the frequency range 1GHz to 7GHz. One-frequency MBPE and two-frequency MBPE are faster than the exact solution for the frequency response calculations.

Comments on CPU time, storage: Though a one-frequency MBPE and a two-frequency MBPE are used in this paper, the rational function can also be evaluated at a number of frequency samples. For example for a rational function of the order (5/4), we need ten frequency samples. This method requires computing the matrix $A(k)$ at ten frequency points. The matrix equation in (13) has to be solved ten times to get the solution vector $e(k)$. At each frequency, only $A(k)$ has to be stored and storage can be reused for all frequencies.

In one-frequency MBPE, to obtain the same order rational function, we need one frequency sample and nine derivatives. This requires computing the matrix $A(k)$ and its nine derivatives at one frequency. In hybrid FEM/MoM technique, the expense of calculating derivative matrices of $A(k)$ is reduced as the derivatives use the terms from the previous derivatives. Also using the direct matrix solver, the matrix $A(k)$ is factored only once and the derivatives of $e(k)$ in equation (28) are obtained by simply backsolving. In this method one needs to store the derivative matrices ($A^{(q)}(k_0)$, $q=1,2,3,...(L+M)$), along with the matrix $A(k_0)$. For electrically large problems, this could impose a burden on computer resources. This problem can be overcome by storing the derivative matrices, $A^{(q)}(k_0)$ out-of-core, as the derivative matrices are required only for matrix-vector multiplication.

Similarly for a two-frequency MBPE we will need two frequency samples and eight derivatives (four at each frequency). In this method, we need to compute $A(k)$ at two frequencies and also four derivatives of $A(k)$ at each frequency. The matrix $A(k)$ is factored once at each frequency and the derivatives of $e(k)$ are obtained by backsolving. In two-frequency MBPE, one needs to store only $([L+M-1]/2)$ derivative matrices along with the matrix $A(k)$ at each frequency. Once the moments are calculated at one frequency, the memory used for the matrices can be reutilized to generate moments at the second frequency, hence reducing the burden on computer memory requirements.

From the above discussion and also from the numerical examples considered in this paper, one-frequency MBPE is

superior in terms of CPU time, whereas it requires the maximum storage. Storage requirements are minimum, if more frequency samples are calculated, than using frequency-derivatives, but CPU time is far more than the one-frequency MBPE or the two-frequency MBPE. In the numerical examples presented with $L=5$ and $M=4$, one-frequency MBPE had to store 10 matrices, whereas two frequency-MBPE had to store 5 matrices at each frequency. The memory to store the matrices at one frequency is reutilized to store the matrices at the second frequency. Hence, even though the CPU timings for two-frequency MBPE is more than the one-frequency MBPE, if computer memory is a constraint, however, it is advisable to use two-frequency MBPE as an alternative to one-frequency MBPE for savings in CPU time and storage requirements.

4 CONCLUDING REMARKS

The MBPE technique is applied to the hybrid FEM/MoM technique to obtain the frequency response of the input characteristics of cavity-backed aperture antennas. The frequency response of input characteristics of an open coaxial line, coaxial cavity, square microstrip patch antenna, and a circular patch antenna are computed and compared with the exact solution. From the numerical examples presented in this work, MBPE technique is found to be superior in terms of CPU time to obtain a frequency response. It may be noted that although calculations are done in frequency increments of 0.1 GHz or 0.01 GHz for the examples presented, the frequency response at even finer frequency increments can also be calculated with a very nominal cost. In one-frequency MBPE the frequency response is valid over a certain frequency range. In two-frequency MBPE, the two frequency values have to be chosen so as to get an accurate frequency response between the two frequency values. To get a wide frequency response for any problem, either one- or two-frequency MBPE models have to be used with different frequency values to cover the complete frequency range. To be accurate over all frequency ranges methods such as adaptive sampling [14] should be applied, which makes MBPE a very effective tool for computational electromagnetics.

APPENDIX

Derivatives of A(k) and b(k) w.r.t. k

The matrix $A(k)$ can be written as (equation 14)

$$A(k) = A_1(k) + A_2(k) + A_3(k) + A_4(k) \tag{A.1}$$

and the qth derivative of $A(k)$ w.r.t. k is given by

$$A^{(q)}(k) = \frac{d^q A(k)}{dk^q} = A_1^{(q)}(k) + A_2^{(q)}(k) + A_3^{(q)}(k) + A_4^{(q)}(k)$$

$$q=0,1,2,3,..... \tag{A.2}$$

Derivatives of $A_1(k)$:

$$A_1^{(0)}(k) = \sum_{jt=1}^{6} \iiint_{mt} \left[(\nabla \times \mathbf{W}_{it}^{(mt)}) \cdot \left(\frac{1}{\mu_r} \nabla \times \mathbf{W}_{jt}^{(mt)} \right) - k^2 \varepsilon_r \mathbf{W}_{it}^{(mt)} \cdot \mathbf{W}_{jt}^{(mt)} \right] dv$$

$$mt=1,2,3,....N_v;\ it=1,2,3,4,5,6 \tag{A.3}$$

$$A_1^{(1)}(k) = -2k\varepsilon_r \sum_{jt=1}^{6} \iiint_{mt} (\mathbf{W}_{it}^{(mt)} \cdot \mathbf{W}_{jt}^{(mt)}) dv$$

$$mt=1,2,3,....N_v;\ it=1,2,3,4,5,6 \tag{A.4}$$

$$A_1^{(2)}(k) = -2\varepsilon_r \sum_{jt=1}^{6} \iiint_{mt} (\mathbf{W}_{it}^{(mt)} \cdot \mathbf{W}_{jt}^{(mt)}) dv$$

$$mt=1,2,3,....N_v;\ it=1,2,3,4,5,6 \tag{A.5}$$

$$A_1^{(q)}(k) = 0 \qquad q \geq 3 \tag{A.6}$$

Derivatives of $A_2(k)$:

$$A_2^{(0)}(k) = \sum_{pt=1}^{N_a} \left[\sum_{lt=1}^{3} \left\{ -\frac{k^2}{2\pi} \iint_{nt} \mathbf{W}_{s(kt)}^{(nt)} \cdot \left(\iint_{pt} \mathbf{W}_{s(lt)}^{(pt)} \frac{\exp(-jkR)}{R} ds' \right) ds \right\} \right]$$

$$nt=1,2,3,....N_a;\ kt=1,2,3 \tag{A.7}$$

$$A_2^{(1)}(k) = \sum_{pt=1}^{N_a} \left[\sum_{lt=1}^{3} \left\{ \iint_{nt} \mathbf{W}_{s(kt)}^{(nt)} \cdot \left(\iint_{pt} \mathbf{W}_{s(lt)}^{(pt)} \left(\frac{j}{2\pi} \right) [2k + k^2(-jR)] \frac{\exp(-jkR)}{(-jR)} ds' \right) ds \right\} \right]$$

$$nt=1,2,3,....N_a;\ kt=1,2,3 \tag{A.8}$$

$$A_2^{(q)}(k) = \sum_{pt=1}^{N_a} \left[\sum_{lt=1}^{3} \left\{ \iint_{nt} \mathbf{W}_{s(kt)}^{(nt)} \cdot \left(\iint_{pt} \mathbf{W}_{s(lt)}^{(pt)} \left(\frac{j}{2\pi} \right) \left[\frac{q!}{(q-2)!} (-jR)^{q-3} + 2qk(-jR)^{q-2} + k^2(-jR)^{q-1} \right] \exp(-jkR) ds' \right) ds \right\} \right] \quad \text{for } q>1$$

$$nt=1,2,3,....N_a;\ kt=1,2,3 \tag{A.9}$$

Derivatives of $A_3(k)$:

$$A_3^{(0)}(k) = \sum_{pt=1}^{N_a}\left[\sum_{lt=1}^{3}\left\{\frac{1}{2\pi}\int\int_{nt}(\nabla\bullet\mathbf{W}_{s(kt)}^{(nt)})\int\int_{pt}(\nabla'\bullet\mathbf{W}_{s(lt)}^{(pt)})\frac{\exp(-jkR)}{R}ds'ds\right\}\right]$$

$$nt=1,2,3,....N_a;\quad kt=1,2,3 \qquad \text{(A.10)}$$

$$A_3^{(q)}(k) = \sum_{pt=1}^{N_a}\left[\sum_{lt=1}^{3}\left\{\frac{1}{2\pi}\int\int_{nt}(\nabla\bullet\mathbf{W}_{s(kt)}^{(nt)})\int\int_{pt}(\nabla'\bullet\mathbf{W}_{s(lt)}^{(pt)})\left(-\frac{j}{2\pi}\right)(-jR)^{(q-1)}\exp(-jkR)ds'ds\right\}\right]$$

$$nt=1,2,3,....N_a;\quad kt=1,2,3 \qquad \text{(A.11)}$$

Derivatives of $A_4(k)$:

$$A_4^{(0)}(k) = \frac{jk\sqrt{\varepsilon_{rc}}}{2\pi\ln\left(\frac{r_2}{r_1}\right)\mu_{rc}}\left[\sum_{rt=1}^{N_i}\left\{\sum_{yt=1}^{3}\left(\int\int_{qt}\mathbf{W}_{xt}^{(qt)}\bullet\left(\frac{\hat{\rho}}{\rho}\right)ds\right)\left(\int\int_{rt}\mathbf{W}_{yt}^{(rt)}\bullet\left(\frac{\hat{\rho}}{\rho}\right)ds'\right)\right\}\right]$$

$$qt=1,2,3,....,N_i;\ xt=1,2,3 \qquad \text{(A.12)}$$

$$A_4^{(1)}(k) = \frac{A_4^{(0)}(k)}{k} \qquad \text{(A.13)}$$

$$A_4^{(q)}(k) = 0 \qquad q \geq 2 \qquad \text{(A.14)}$$

Derivatives of $B(k)$:

$$B(k) = \frac{2jk\sqrt{\varepsilon_{rc}}\exp(-jk\sqrt{\varepsilon_{rc}}z_1)}{\mu_{rc}\sqrt{2\pi\ln\left(\frac{r_2}{r_1}\right)}}\int\int_{qt}\mathbf{W}_{xt}^{(qt)}\bullet\left(\frac{\hat{\rho}}{\rho}\right)ds$$

$$qt=1,2,3,.....N_i;\quad xt=1,2,3 \qquad \text{(A.15)}$$

$$B^{(q)}(k) = (-j\sqrt{\varepsilon_{rc}}z_1)^q\left[1-\frac{q}{jk\sqrt{\varepsilon_{rc}}z_1}\right]B^{(0)}(k) \qquad \text{(A.16)}$$

Equation (A.16) is written in a compact form, however, it must be simplified before evaluating at $z_1 = 0$.

REFERENCES

[1] J. M. Jin and J. L. Volakis, "A hybrid finite element method for scattering and radiation by microstrip patch antennas and arrays residing in a cavity," *IEEE Trans. Antennas and Propagation*, Vol.39, pp.1598-1604, November 1991.

[2] C. J. Reddy, M. D. Deshpande, C. R. Cockrell and F. B. Beck, "Radiation characteristics of cavity backed aperture antennas in finite ground plane using the hybrid FEM/MoM technique and geometrical theory of diffraction," *IEEE Trans. Antennas and Propagation*, Vol.44, pp.1327-1333, October 1996.

[3] E.K.Miller and G.J.Burke, "Using model-based parameter estimation to increase the physical interpretability and numerical efficiency of computational electromagnetics," *Computer Physics Communications*, Vol.68, pp.43-75, 1991.

[4] G.J.Burke, E.K.Miller, S.Chakrabarthi and K.Demarest, "Using model-based parameter estimation to increase the efficiency of computing electromagnetic transfer functions," *IEEE Trans. Magnetics*, Vol.25, pp.2807-2809, July 1989.

[5] G.J.Burke, "Enhancements and limitations of the code NEC for modeling electrically small antennas," *Lawrence Livermore National Laboratory, UCID-20970*, January 1987.

[6] C.J.Reddy, "Application of model based parameter estimation for fast frequency response calculations of input characteristics of cavity-backed aperture antennas using hybrid FEM/MoM technique," *NASA Contractor Report-1998-206950*, March 1998.

[7] J.M.Jin, *Finite Element Method in Electromagnetics*, John Wiley & Sons, 1993.

[8] E. Chiprout and M. S. Nakhla, *Asymptotic Waveform Evaluation*, Kulwar Academic Publishers, 1994.

[9] C.J.Reddy, M.D.Deshpande, C.R.Cockrell and F.B.Beck, "Fast RCS computation over a frequency band using the combined FEM/MoM technique in conjunction with Asymptotic waveform evaluation(AWE)," to appear in *Electromagnetics*, 1998.

[10][1] C.R.Cockrell and F.B.Beck, "Asymptotic Waveform Evaluation (AWE) technique for frequency domain electromagnetic analysis," *NASA Technical Memorandum 110292*, November 1996.

[11][1]C.J.Reddy and M.D.Deshpande, "Frequency response calculations of input characteristics of cavity-backed aperture antennas using AWE with hybrid FEM/MoM technique," *NASA Contractor Report 4764*, February 1997.

[12][2]C.J.Reddy and M.D.Deshpande, "User's Manual for CBS3DR-Version 1.0," *NASA Contractor Report 198284*, February 1996.

[13] O. O. Storaasli, "Performance of NASA equation solvers on computational mechanics applications," *American Institute of Aeronautics and Astronautics (AIAA) Paper No. 96-1505*, April, 1996.

[14] E.Miller, "Computing radiation and scattering patterns using model-based parameter estimation," *1998 IEEE Antennas and Propagation Society International Symposium Digest*, Volume 1, pp. 66-69, June 1998.

1. Available through NASA Technical Report server at *http://techreports.larc.nasa.gov/ltrs/ltrs.html*
2. CBS3DR code is distributed by NASA Langley Research Center, Hampton VA 23681, USA